ISSN 1674-1056
http://cpb.iphy.ac.cn
http://iopscience.iop.org/cpb
中国物理 B
Chinese Physics
中国物理 Chinese Physics B

Cascaded tilted fiber Bragg grating for enhanced refractive index sensing

Biqiang Jiang(姜碧强), Zhixuan Bi(毕芷瑄), Shouheng Wang(王守恒), Teli Xi(席特立), Kaiming Zhou, Lin Zhang, Jianlin Zhao(赵建林)

Citation: Chin. Phys. B . 2018, 27(11): 114220. **doi:** 10.1088/1674-1056/27/11/114220

Journal homepage: http://cpb.iphy.ac.cn; http://iopscience.iop.org/cpb

What follows is a list of articles you may be interested in

Ultrasonic sensitivity-improved fiber-optic Fabry-Perot interferometer using a beam collimator and its application for ultrasonic imaging of seismic physical models

Zhi-Hua Shao(邵志华), Xue-Guang Qiao(乔学光), Feng-Yi Chen(陈凤仪), Qiang-Zhou Rong(荣强周)

Chin. Phys. B . 2018, 27(9): 094218. **doi:** 10.1088/1674-1056/27/9/094218

Performance analysis of surface plasmon resonance sensor with high-order absentee layer

Qing-Qing Meng(孟庆卿), Xin Zhao(赵鑫), Shu-Jing Chen(陈淑静), Cheng-You Lin(林承友), Ying-Chun Ding(丁迎春), Zhao-Yang Chen(陈朝阳)

Chin. Phys. B . 2017, 26(12): 124213. **doi:** 10.1088/1674-1056/26/12/124213

Gamma-radiation effects in pure-silica-core photonic crystal fiber

Wei Cai(蔡伟), Ningfang Song(宋凝芳), Jing Jin(金靖), Jingming Song(宋镜明), Wei Li(李伟), Wenyong Luo(罗文勇), Xiaobin Xu(徐小斌)

Chin. Phys. B . 2017, 26(11): 114211. **doi:** 10.1088/1674-1056/26/11/114211

Effect of radiation-induced color centers absorption in optical fibers on fiber optic gyroscope for space application

Jing Jin(金靖), Ya Li(李亚), Zu-Chen Zhang(张祖琛), Chun-Xiao Wu(吴春晓), Ning-Fang Song(宋凝芳)

Chin. Phys. B . 2016, 25(8): 084213. **doi:** 10.1088/1674-1056/25/8/084213

High refractive index sensitivity sensing in gold nanoslit arrays

Yuan Jun, Kan Qiang, Geng Zhao-Xin, Xie Yi-Yang, Wang Chun-Xia, Chen Hong-Da

Chin. Phys. B . 2014, 23(8): 084201. **doi:** 10.1088/1674-1056/23/8/084201

SPECIAL TOPIC — 80th Anniversary of Northwestern Polytechnical University (NPU)

Cascaded tilted fiber Bragg grating for enhanced refractive index sensing*

Biqiang Jiang(姜碧强)[1,2,†], Zhixuan Bi(毕芷瑄)[1], Shouheng Wang(王守恒)[1], Teli Xi(席特立)[1], Kaiming Zhou[2], Lin Zhang[2], and Jianlin Zhao(赵建林)[1]

[1] *MOE Key Laboratory of Material Physics and Chemistry under Extraordinary Conditions and Shaanxi Key Laboratory of Optical Information Technology, School of Science, Northwestern Polytechnical University, Xi'an* 710072, *China*

[2] *Aston Institute of Photonic Technologies, Aston University, Birmingham B4 7ET, UK*

(Received 17 July 2018; revised manuscript received 2 September 2018; published online 8 October 2018)

We proposed and experimentally demonstrated a cascaded tilted fiber Bragg grating (TFBG) for enhanced refractive index sensing. The TFBG is UV-inscribed in series in ordinary single-mode fiber (SMF) and reduced-diameter SMF with the same tilt angle, and then excites two sets of superposed spectral combs of cladding modes. The cascaded TFBG with total length of 18 mm has a much wider wavelength range over 100 nm and narrower wavelength separation than that of a TFBG only in the SMF, enabling an enlarged range and a higher accuracy of refractive index measurement. The fabricated TFBG with the merits of enhanced sensing capability and temperature self-calibration presents great potentials in the biochemical sensing applications.

Keywords: tilted fiber Bragg grating, fiber optics sensors, refractive index measurement

PACS: 42.81.Pa, 42.79.–e, 42.81.Qb, 42.81.–i **DOI:** 10.1088/1674-1056/27/11/114220

1. Introduction

Surrounding refractive index (SRI) and temperature measurements are very important in various fields such as biochemical industry, environmental monitoring, and life science. Recently, optical fiber-based SRI sensors have attracted more interests because of their advantages of compact structure, remote interrogation, high sensitivity, etc. Tilted fiber Bragg gratings (TFBGs) belong to the short-period grating family, but the grating planes are slanted with respect to the fiber axis. The slanted grating planes can make the light propagating in the fiber core penetrate to the cladding even to much deeper surrounding medium, without any requirement of special alteration in the fiber cladding, such as etching, side-polishing, etc. TFBGs can therefore be used as SRI sensors with the combinations of advantages in mature fiber Bragg grating technology and resonant excitations of cladding modes, providing a promising structure for SRI sensing.[1] Based on the above merits, the TFBGs have been applied in the sensing of many parameters that can be converted to the measurement of SRI.[2–7] In the meantime, the core mode resonance provides an absolute power and wavelength reference, which can therefore be used to eliminate uncertainties such as the power fluctuation of the light source and the variation of the ambient temperature.[1,8]

The tilt angle of a TFBG is an important parameter, which can determine the spectrum range of the cladding modes and the SRI measurement range. For the TFBG with a small tilt angle, it usually is highly sensitive in the SRI region above 1.4.[9–12] For covering the lower SRI region such as the refractive index of water where most biochemical applications require, it is a common method to increase the tilt angle of the TFBG.[1,13] Another way is to coat some materials onto the TFBG surface. For instance, by coating the TFBG with a gold film to excite surface plamon resonance and smartly using its polarized spectral information, the SRI measurement range can be effectively extended even to air.[14–17] By integrating carbon nanomaterials with complex refractive index such as graphene or carbon nanotube onto the TFBG, the sensing capacity in the low refractive index region can also be enhanced based on the interaction between the nanomaterials and the cladding modes.[9,18,19]

In this work, we report a cascaded TFBG with the tilt angle of 6.5° in ordinary single-mode fiber (SMF) and reduced-diameter SMF (RD-SMF) for the enhancement of the SRI sensing performance, without any coating or larger tilt angle. Excitation and superposition of two sets of cladding mode resonances will broaden the spectral range over 100 nm and reduce the separation between the cladding modes, achieving the enlarged range and enhanced accuracy of the SRI measurement. In addition, we investigate the SRI response in the range of 1.30–1.45, and obtain the sensitivities of 510.48 nm/RIU and 494.12 nm/RIU in different SRI regions. The fabricated

*Project supported by the National Natural Science Foundation of China (Grant Nos. 61775182 and 61505165) and Marie Skłodowska-Curie Individual Fellowships in the European Union's Horizon 2020 Research and Innovation Programme (Grant No. 660648).

†Corresponding author. E-mail: bqjiang@nwpu.edu.cn

© 2018 Chinese Physical Society and IOP Publishing Ltd

TFBG with a small tilt angle can achieve a wide range of SRI measurement, and has the potentials in the applications such as biochemical and environmental sensing.

2. Principle

Figure 1 depicts a schematic diagram of the cascaded TFBG structure for SRI measurement. It is well known that in a standard FBG, the only strong coupling permitted occurs between the forward and backward-propagating core modes, for which the light is confined near the fiber axis and isolated from the surroundings by the relative thick cladding.[20] However, for a TFBG, the tilted fringes can improve the light coupling from the forward-propagating core mode to the backward-propagating cladding modes at shorter wavelengths, and simultaneously reduce the coupling of the backward-propagating core mode. According to the phase-matching conditions, the resonant wavelengths of the backward coupled core (λ_{co}) and cladding (λ_{cl}) modes of the TFBG can be expressed as follows:

$$\lambda_{co} = 2n_{eff}^{co}(\lambda_{co})\Lambda/\cos\theta, \tag{1}$$

$$\lambda_{cl} = \left[n_{eff}^{co}(\lambda_{cl}) + n_{eff}^{cl}(\lambda_{cl})\right]\Lambda/\cos\theta, \tag{2}$$

where Λ is the nominal grating period, θ is the tilt angle of the grating planes with respect to the fiber cross-section, $n_{eff}^{co}(\lambda_{co})$ and $n_{eff}^{co}(\lambda_{cl})$ are the effective indices of the core mode at the wavelengths of λ_{co} and λ_{cl}, respectively, and $n_{eff}^{cl}(\lambda_{cl})$ is the effective index of the cladding mode at λ_{cl}. According to Eqs. (1) and (2), apart from the tilt angle θ, the core mode and the cladding modes are determined by the refractive indices of the fiber core and cladding. As a result, we can adjust the spectral range by inscribing the grating in different types of fibers with different parameters.

For a specific cladding mode, if its effective index is lower than the SRI, the cladding modes will no longer be confined in the fiber cladding, leaking into the surrounding medium. However, if the effective index is higher than the SRI, the cladding mode is totally confined by the relative thick cladding. When the effective index is equal to the SRI, regarding as a cutoff state, the wavelength of the cladding mode is marked as a cutoff wavelength, which is analogous to the critical angle of an Abbe refractometer.[21]

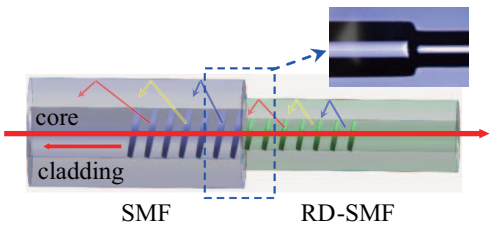


Fig. 1. (color online) Schematic model of the cascaded TFBG. The inset is the photograph of the splicing joint between the SMF and RD-SMF.

3. Fabrication and characteristics of the cascaded TFBG

In the device fabrication, a segment of 15 mm long RD-SMF was spliced between standard SMFs by a fiber arc fusion splicer. The core/cladding diameter of the employed RD-SMF is approximately 3.8/80 μm. As displayed in the inset of Fig. 1, due to the smaller diameter, the arc power and arc time need to be adjusted for low splice loss. The photosensitivity of SMF and RD-SMF was firstly enhanced by H_2 loading for 72 h. After splicing and hydrogenation, the TFBG was UV-inscribed in series in the SMF and RD-SMF by using a frequency doubled continuous wave Ar^+ laser of 244 nm wavelength with the help of scanning phase-mask technique. The lengths of TFBG in SMF and RD-SMF are 8 mm and 10 mm, respectively. The tilt angle of the grating plane is about 6.5° , and the grating period is 543.8 nm determined by the phase mask. The fabricated cascaded TFBG was annealed at 80 °C for 48 h to release the residual hydrogen and stabilize the grating structure.

We characterized the transmission spectrum of the cascaded TFBG by an experimental system, including a supercontinuum (superK) light source and an optical spectrum analyzer (OSA). Launched from the superK source, the broadband light covering the spectrum range of 1400–1600 nm was transmitted into the cascaded TFBG, and the transmission spectrum was monitored and recorded by the OSA with a minimum wavelength resolution of 0.02 nm. The measured spectrum of the cascaded TFBG around the air is depicted at the top of Fig. 2(a). We can clearly observe a relative wide spectrum ranging from 1460 nm to 1560 nm held by the cladding mode resonances of the cascaded TFBG. As a comparison, the TFBGs with the same tilt angle and grating length only in the SMF and RD-SMF are shown at the bottom of Fig. 2(a). Clearly, if a TFBG with the same tilt angle of 6.5° is fabricated in the standard SMF, the cladding modes can only be excited in the spectrum range of 1500–1550 nm.

As the discreteness of the cladding modes will reduce the measurement accuracy of the SRI, we tracked the separations of the adjacent mode resonances of the TFBGs in SMF and RD-SMF and cascaded TFBG, and the results are shown in Fig. 2(b). The separation between the adjacent resonances changes with the wavelength, and a larger separation appears at the shorter wavelength region. And also, the separation of the TFBG in SMF is smaller than that of the TFBG in RD-SMF. However, in the spectral region of 1500–1550 nm, the separation for the cascaded TFBG is mainly determined by that of the TFBG in SMF and periodically modulated by that of the TFBG in RD-SMF, and thus exhibits a periodical vibration, instead of the original exponential change with the wavelength. On the whole, the separation of the cascaded TFBG

becomes smaller due to the superposition of the transmission spectra of the TFBGs in SMF and RD-SMF. Therefore, the measurement range will be expanded by the broader spectrum range of the TFBG, and also the measurement uncertainty will be reduced by the smaller separation of the comblike spectrum.

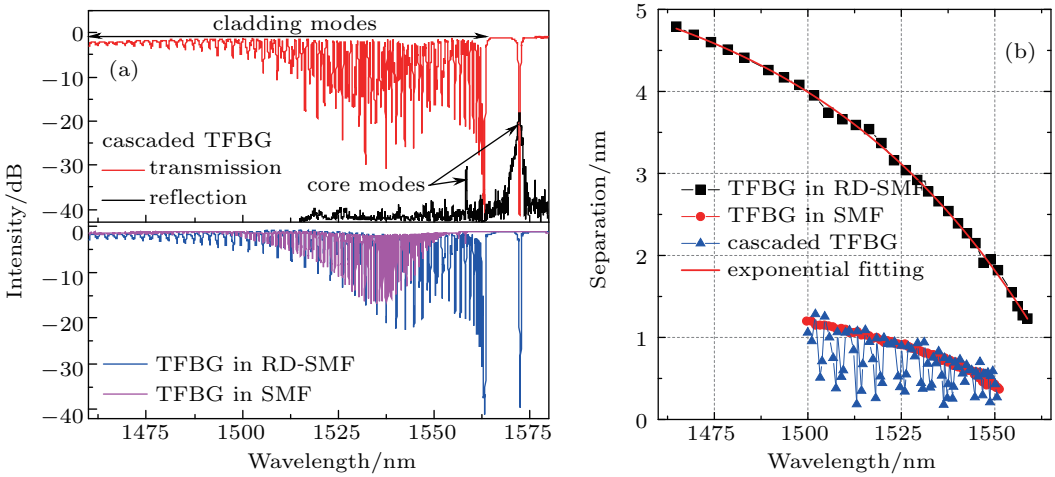


Fig. 2. (color online) (a) Measured transmission spectra of the cascaded TFBG (top with red line) and the TFBGs (bottom) with the same tilt angle in SMF (with magenta line) and RD-SMF (with blue line); (b) separations of adjacent cladding mode resonances at different wavelengths of the TFBGs.

4. Experimental results and discussion

4.1. Refractive index response

In the experiment, we use the experimental system as described in the report[22] to examine the SRI response of the cascaded TFBG. The broadband light from the superK source is coupled in the TFBG, and the transmission signal is monitored and recorded by the OSA. And then, a series of refractive index matching liquids with the range of 1.300–1.450 and the interval of 0.005 are injected into the sample cell in turn to change the SRI around the TFBG.

Figure 3(a) demonstrates the spectral evolution of the cascaded TFBG with SRI variation, and the position of cutoff mode resonance at each SRI is indicated with the red asterisk. The so-called cutoff mode is located between the leaky and guided modes, which is evidenced by an apparent reduction of coupling intensity compared with the guided cladding mode at the longer wavelength side.[21,23,24] According to the total internal reflection condition, the effective indices of the cladding modes are lower than that of the surrounding medium, and then the cladding modes are no longer confined by the fiber cladding, evolving into dissipative leaking modes. The cutoff mode is usually used for the SRI measurement due to the high sensitivity compared to other guided cladding modes or leaky modes, and it monotonically moves towards the longer wavelength as the SRI increases.[13]

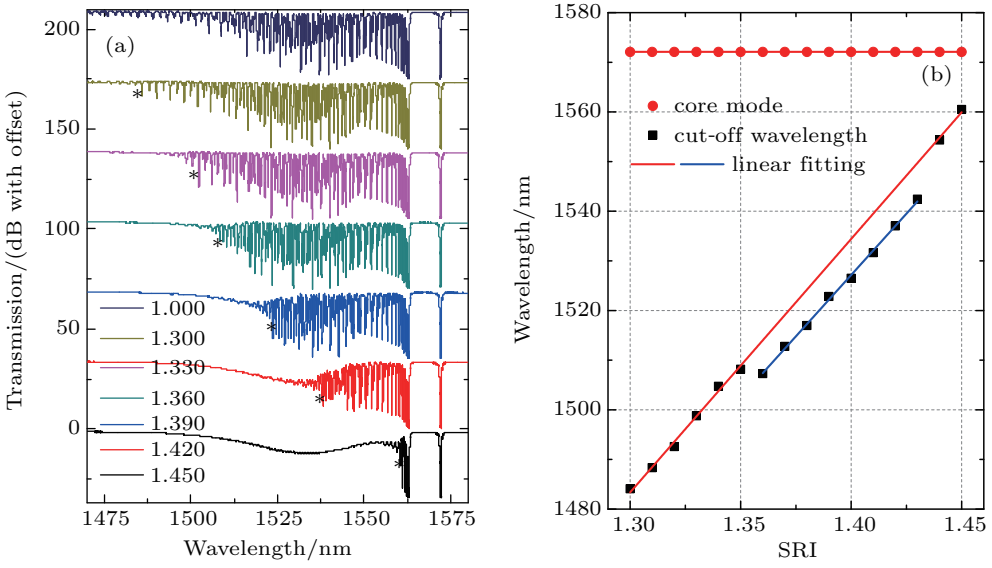


Fig. 3. (color online) (a) Spectral evolution of the cascaded TFBG with the SRI change, and (b) the extracted wavelengths of the core mode and cut-off mode resonances versus the SRI.

From the spectral evolution of the cascaded TFBG shown in Fig. 3(a), we extracted the wavelengths of the cutoff mode resonances at each SRI, as shown in Fig. 3(b). Clearly, the curve of cutoff wavelength versus SRI is divided into two parts. In the upper part of the curve, the cutoff wavelength is only determined by the cladding modes of TFBG in RD-SMF, while in the lower part, corresponding to the SRI region of 1.36–1.43, the cutoff wavelength is determined by the superposed cladding modes due to the concatenation of two TFBGs. After linear fitting, the slopes of lower and upper parts in the SRI response curve are 510.48 nm/RIU (RIU represents the refractive index unit) with R^2 of 0.9994 and 494.12 nm/RIU with R^2 of 0.9985, respectively. According to Eq. (2), the difference of the slope originates from the different effective indices of the core and cladding modes in two types of optical fibers. For real measurement, it is therefore essential to choose the corresponding response coefficients for different SRI regions, and easy to locate the SRI region according to the position of the cutoff wavelength in the spectrum. More importantly, by employing the cascaded TFBG, the SRI sensing is enlarged to the range of 1.30–1.45. While, a 6.5° TFBG in SMF can only sense the SRI in the range of 1.36–1.43. Considering the discreteness of cladding modes of the cascaded TFBG, we can use the finer wavelength shift of cutoff mode resonance as "vernier" scale to further improve the measurement accuracy, which is reported in our previous work.[24] Moreover, the core mode of the cascaded TFBG always remians unchanged with the SRI variation, and then its wavelength can be used a reference to eliminate the effect of the ambient temperature fluctuation.

4.2. Temperature response

The change of the temperature around the cascaded TFBG will affect the grating period and the effective indices of the core mode and cladding modes via thermal expansion and thermal-optic effects, as a result, the transmission spectrum of the TFBG will globally shift with temperature. Then, we experimentally investigated the temperature response by placing the TFBG in a temperature-controllable heating chamber with a calibrated temperature probe. We heated the TFBG from 0 °C to 80 °C, and recorded the spectrum in the interval of 10 °C. Different from the SRI response results, as the temperature increases, the spectral evolution demonstrates a constant coupling intensity but shifted resonant wavelength. Figure 4 shows the wavelength shifts of different mode resonances. The core mode at the resonant wavelength of around 1572 nm, and the cladding modes at different wavelengths of 1560 nm, 1530 nm, 1501 nm, and 1469 nm shift linearly and simultaneously with the temperature, and their response coefficients are 11.83 pm/°C, 11.29 pm/°C, 11.02 pm/°C, 10.90 pm/°C, and 10.69 pm/°C, respectively. The cascaded TFBG has a smaller temperature response coefficient at the shorter wavelength. Therefore, the SRI and ambient temperature can be simultaneously acquired by extracting the wavelengths of the core mode and cutoff mode resonances.

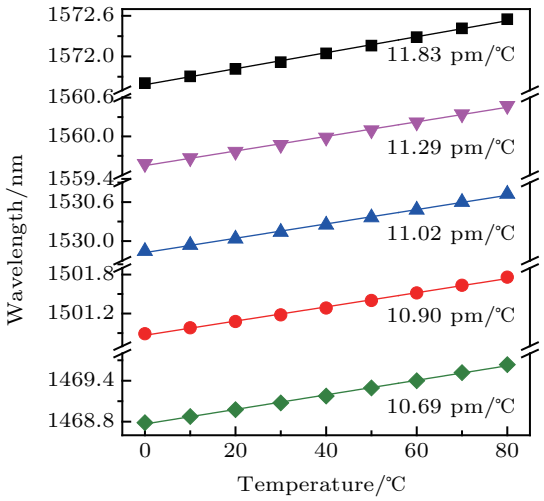


Fig. 4. (color online) (a) Wavelength shifts of the core mode and the cladding modes with the temperature increasing.

5. Conclusion

We proposed, fabricated, and demonstrated a cascaded TFBG with two sets of cladding mode resonances for enhanced SRI sensing performance. Relying on the broad spectrum range of more than 100 nm of the cascaded TFBG, the SRI sensing range can be effective extended to 1.30–1.45. Meanwhile, by tracking the cutoff mode and core mode resonances, the SRI and temperature can be simultaneously obtained according to the strictly linear responses to temperature and SRI. The response coefficients of the temperature and SRI are 11.83 pm/°C and 510.48 nm/RIU (or 494.12 nm/RIU), respectively. Therefore, the cascaded TFBG in SMF and RD-SMF with rich spectral properties and enhanced sensing capacity could be desirable in-fiber devices for biochemical sensing, environmental monitoring, and other signal processing applications.

References

[1] Albert J, Shao L Y and Caucheteur C 2013 *Laser Photon. Rev.* **7** 83
[2] Guo T, Liu F, Liu Y, Chen N K, Guan B O and Albert J 2014 *Biosens. Bioelectron.* **55** 452
[3] Guo T, Liu F, Guan B O and Albert J 2016 *Opt. Laser Technol.* **78** 19
[4] Yang D, Du L, Xu Z, Jiang Y, Xu J, Wang M, Bai Y and Wang H 2014 *Appl. Phys. Lett.* **104** 061903
[5] Voisin V, Pilate J, Damman P, Mégret P and Caucheteur C 2014 *Biosens. Bioelectron.* **51** 249
[6] Wang Y, Shen C, Lou W, Shentu F, Zhong C, Dong X and Tong L 2016 *Appl. Phys. Lett.* **109** 031107
[7] Shen C, Zhong C, Liu D, Lian X, Zheng J, Wang J, Semenova Y, Farrell G, Albert J and Donegan J F 2018 *Opt. Lett.* **43** 255

[8] Guo T, González-Vila Á Loyez M and Caucheteur C 2017 *Sensors* **17** 2732
[9] Jiang B, Lu X, Gan X, Qi M, Wang Y, Han L, Mao D, Zhang W, Ren Z and Zhao J 2015 *Opt. Lett.* **40** 3994
[10] Gu B, Qi W, Zheng J, Zhou Y, Shum P P and Luan F 2014 *Opt. Lett.* **39** 22
[11] Shi X, Zheng S, Chi H, Jin X and Zhang X 2012 *Opt. Express* **20** 10853
[12] Wang T, Liu K, Jiang J, Xue M, Chang P and Liu T 2017 *Opt. Express* **25** 14900
[13] Chen X, Xu J, Zhang X, Guo T and Guan B O 2017 *IEEE Photon. Technol. Lett.* **29** 719
[14] Shen C, Zhang Y, Zhou W and Albert J 2014 *Appl. Phys. Lett.* **104** 071106
[15] González-Vila Á Ioannou A, Loyez M, Debliquy M, Lahem D and Caucheteur C 2018 *Opt. Lett.* **43** 2308
[16] Caucheteur C, Guo T, Liu F, Guan B O and Albert J 2016 *Nat. Commun.* **7** 13371
[17] Caucheteur C, Shevchenko Y, Shao L Y, Wuilpart M and Albert J 2011 *Opt. Express* **19** 1656
[18] Jiang B, Lu X, Mao D, Wang Y, Zhang W, Gan X and Zhao J 2016 *IEEE Photon. Technol. Lett.* **28** 994
[19] Villanueva G E, Jakubinek M B, Simard B, Otón C J, Pérez-Millán P and Albert J 2011 *CLEO/Europe-EQEC*
[20] Albert J 2011 *Opt. Photon. News* **22** 28
[21] Zhou W, Mandia D J, Barry S T and Albert J 2015 *Opt. Lett.* **40** 1713
[22] Jiang B, Lu X, Mao D, Zhang W and Zhao J 2015 *IEEE Sens. J.* **15** 3000
[23] Zhou W, Zhou Y and Albert J 2017 *Laser Photon. Rev.* **11** 1600157
[24] Jiang B, Zhou K, Wang C, Zhao Y, Zhao J and Zhang L 2017 *Opt. Express* **25** 25910